

FIRE IN TARGETING URBAN/INDUSTRIAL AREAS

H. L. Brode and R. D. Small

Pacific-Sierra Research Corporation
12340 Santa Monica Boulevard
Los Angeles, California 90025

AD P001817

ABSTRACT

A preliminary study of the parameters pertinent to considerations of fire in urban targeting illustrated the dominance of some factors and the insensitivity to damage assessments of others. The factors considered, together with the simple assumptions and approximations used in this scoping study supported the assumption that fire may add significantly to the damage to urban/industrial targets. The influence of uncertainties and unknowns were evaluated, and the consequent implications for research were assessed. This work was done in cooperation with RDA (R. Port) for DNA.

INTRODUCTION

Damage from a nuclear weapon burst is usually associated with the blast wave, nuclear radiation, electromagnetic pulse and thermal radiation. Theoretical or empirical relations describing shock wave propagation, diffusion of nuclear radiation and transmission of thermal and electromagnetic radiation are well developed. Translation of each effect to a damage prediction requires analysis of the target response. In general, the correlation of the weapon effect with target damage is non-linear and complex. Most current damage estimates are based on relations describing structural response to shock wave loadings. No such correlations are available to define fire damage.

In general, the prediction of fire damage is no more complex than the prediction of blast damage. The loading and damage of a structure by the blast wave is a complex function of orientation, timing, and strengths of materials. Fire in a target building may develop from ignitions due to thermal loadings or from blast disruption, or from spread from an adjacent burning building. The first two mechanisms relate to weapon effects. Spread relates to established adjacent fires, so that the immediate weapon effect-target response provides only a partial fire damage estimate. Description of the fire development and later time behavior is necessary for a complete damage prediction. Both the immediate weapon effect-target response and the effect of many unchecked fires in a city must be analyzed.

In this paper, many of the factors that may influence the occurrence and development of fires in a target area are considered, and probability of fire damage-range curves are constructed. The analysis includes available relations and criteria for transmission of thermal radiation, ignition criteria, and blast induced ignitions. Fire spread and civil defense actions are approximated. In most cases, a parameter range was created in order to compensate for either a lack of data or an inadequate prediction methodology. Conservative estimates of the parameter values indicate a damage range greater than that for light blast damage. Less conservative estimates produce fire damage radii greatly exceeding comparable blast damage radii.

FIRE DAMAGE RANGE CURVES

THERMALLY-INDUCED IGNITIONS

The basic fire damage-range relation is based on the probability of occurrence of a sustainable ignition. Considering heavy drapes, bedding and overstuffed furniture as representative combustible materials, then for a 1 Mt burst, ignition is likely at a flux level of 22 cal/cm² (1). For that value, a target fire resulting in structure destruction is assumed 50% probable. A 90% probability is assumed for 33 cal/cm², and a 10% probability for 11 cal/cm². The ignition threshold levels increase slowly with weapon yield.

Slant ranges and thus damage (ground) ranges for each threshold level (Q) are calculated from

$$S = \left[\frac{W}{Q} (1 + \beta S/V) e^{-\alpha S/V} \right]^{1/2} \text{ mi} .$$

The weapon yield is W (kt), and Q is in cal/cm², V is the visibility length (mi) and α , β define the scattering and absorption characteristics of the atmosphere. The basic fire damage-range curve for thermally induced ignitions is shown in Fig. 1. The values 2.0, 1.4 chosen for α , β are recommended by Brode (2). Damage ranges are reduced slightly (3) for α , $\beta = 2.9, 1.9$ (4). A much greater influence is the characteristic visibility length. The 50% damage radius increases by a factor of two for the visibility length range of 3 to 48 miles. The variation depends on weapon yield--decreasing for lower yields (3).

The amount of thermal radiation incident on a target may be enhanced by reflection from a ground snow cover or superior cloud deck or attenuated by cloud cover below the burst. A simple multiplicative constant (greater than 1.0 for enhancement, less than 1.0 for attenuation) is used to estimate the influence on damage ranges. Sample results are shown in Fig. 2. Reflection of thermal radiation can increase the damage range by 30%. The thermal reach is halved if 75% of the fireball radiation is absorbed by a cloud layer.

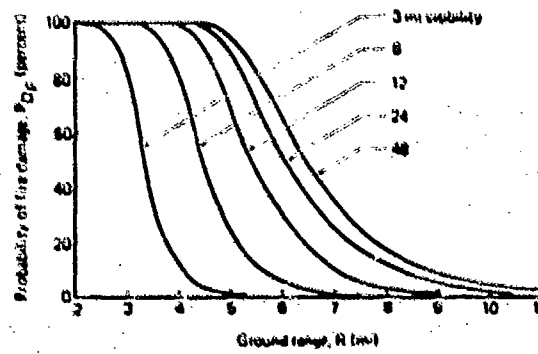


Fig. 1 Fire damage range for various visibility lengths. Thermally induced ignitions, $W = 1 \text{ Mt}$, $Q = 22 \text{ cal/cm}^2$

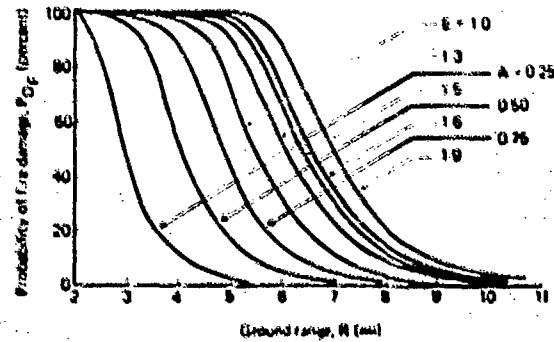


Fig. 2 Fire damage range for various atmospheric conditions. $E = 10, 13, 15, 16, 0.50, 0.75, 1.0$ (see 20, p. 1-6)

Other factors that may influence the damage-range relation include height of burst and threshold level variations (3). With the exception of ground bursts, the height of burst modifies the results only slightly (less than 5% for scale burst heights between 200 ft/kt^{1/3} and 700 ft/kt^{1/3}). Significant changes occur for increased or decreased threshold levels. A 50% decrease in threshold levels doubles the damage areas. Variation of the 10 and 90% values sharply slew the damage range curves. These parameters have been considered in detail by Brode and Small (3).

BLAST-INDUCED IGNITIONS

The blast wave from a nuclear burst may disrupt electrical, open flame and other high-energy fuel sources, starting a substantial number of fires. The methodology of Wilton, Myonuk and Zaccor (5) is used to estimate the probability of a fire start as a function of overpressure, structure type and contents. The applicability of this model may be limited by its assumptions, however, the resulting probabilities agree fairly well with those suggested by the large burned-out regions of Hiroshima and Nagasaki (6, 7).

Figure 3 plots sample fire damage-range curves for several combinations of building types and contents. A light-design structure (type 10) with highly flammable contents (approaching 10) presents a high probability of blast induced fires beyond the 0.5 psi level (13 to 24 miles for a 1 Mt burst). Each damage-range curve assumes a uniform building-contents distribution throughout the target area. Damage ranges shown for the light design structures greatly exceed those for thermally induced ignitions. For those cases, blast-induced fire starts dominate the ignition distribution, and variations in visibility length or the coefficients α , β cannot greatly affect the damage ranges.

COMBINED PROBABILITIES

The damage range curves in Fig. 4 combine the probabilities of ignition by thermal radiation and blast. The indices for building type and contents are fixed (4/7.5) at all ranges, ensuring a homogeneous distribution of buildings. Combining the independent probabilities of thermally and blast-induced ignitions significantly extends the damage-range curves. However, attenuation of the incident thermal energy reduces the probable damage range just slightly, whereas enhancement moderately increases the damage range. Lower building type/contents indices would shift the curves to the left. Inclusion of blast-induced ignitions in the computation of probable fire starts lessens the influence of the visibility length and the attenuation or enhancement of thermal radiation. Those parameters would be more important, however, if the distribution of blast-induced ignitions (as shown in Fig. 4) has been overestimated.

A more specific analysis of the sources of blast-induced fires in Soviet cities would be valuable. Such sources may be electrical, thermal, chemical, mechanical, electrostatic, or gas dynamic. Certain industries, such as paper mills, chemical plants, oil refineries, or power generators, contain obvious potential secondary sources, and could be targeted accordingly. Such features, when identifiable, should be part of the vulnerability considerations, since the ensuing fires are likely to extensively damage some facilities that might otherwise survive the blast. Such was the case for an electric generating station in Hiroshima--though housed in a massive building that survived the blast, the station itself was gutted by fire.

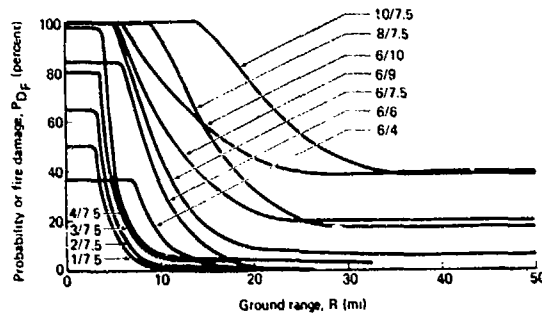


Fig. 3 Fire damage range for various building type/contents indices: blast-induced ignitions, $W = 1 \text{ Mt}$.

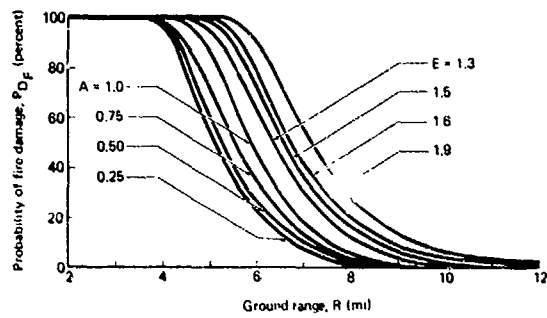


Fig. 4 Fire damage range for various amounts of radiation attenuation A and enhancement E: thermally and blast-induced ignitions, $W = 1 \text{ Mt}$, $V = 12 \text{ mi}$, $d = 2.0$, $\theta = 1.4$, building type/contents index = 4/7.5.

FIRE SPREAD

When many simultaneous fires are ignited in conjunction with considerable blast damage and radioactive fallout, the best civil defense efforts cannot hope to contain them. The added threat of multiple or sequential bursts will further deter effective firefighting. Under those circumstances, fire spread is limited chiefly by natural boundaries (rivers, lakes) or man-made barriers (open areas such as parks, parking lots, broad boulevards). However, even such firebreaks have not always proved effective against a large fire. The ultimate limit is the fuel bed itself; when there is no more fuel to burn, the fire must stop. Within densely constructed areas, industrial facilities with highly flammable contents, or extensively damaged regions with widely scattered debris, fire is more likely to spread. Contiguous fuel sources are likely to burn completely once numerous fires are started and civil services disrupted.

Consistent with the previous assumptions of our simple, generic fire damage model, a heuristic accounting for fire spread is used. Thus, the model ignores a continuity of structures and the flammability of their contents, the direction of winds and blast waves, and the potential for flammable debris, though all could significantly affect fire spread. Regions between multiple bursts will suffer fire damage, because of a tendency of large fires ignited by multiple bursts to merge with neighboring fires.

Fire spread was included in the damage-range relation by doubling the probability of a fire at each point. Thus, if 50% of the structures are burning, it is assumed that the fire will spread to all adjacent structures. Similarly, ignition in one building in four implies fire damage to 50% of the structures. Results of those calculations are plotted in the fire-damage-range curve in Fig. 5, which combines the probabilities of ignition by thermal radiation and blast, followed by fire spread. The

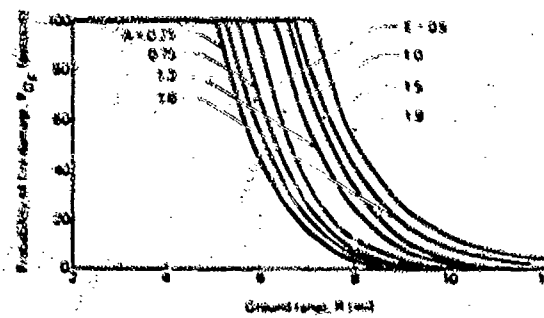


Fig. 5 Fire damage range for various amounts of radiation attenuation A and enhancement E: thermally and blast-induced ignitions and fire spread, $W = 1 \text{ Mt}$, $V = 12 \text{ mi}$, $d = 2.0$, $\theta = 1.4$, building type/contents index = 4/7.5.

modifying effects of enhancement and attenuation of the thermal radiation are also incorporated. At even the largest attenuation factor, complete fire damage extends to the 3 psi region (5 mi for 1 Mt).

COMBINED PARAMETER VARIATIONS

This section develops fire-damage-range curves for multiple-parameter combinations. The nine "independent" variables considered include ignition threshold level, visibility length, transmissivity form, thermal radiation enhancement and attenuation, building type/contents indices for blast-induced fires, probability of fire spread, and the effectiveness of countermeasures against thermally and blast-induced ignitions. Based on the previous parameter excursions, a mean value for each variable was defined. One- and two-standard-deviation bracketing values were then estimated. Interpolation between the mean and $\pm 1\sigma$ deviation ensembles was used to define $\pm 1/3\sigma$ and $\pm 2/3\sigma$ values for each variable (unit standard deviations). The nine "independent" variables were then combined to form $\pm 1\sigma$ and $\pm 2\sigma$ fire-damage-range curves for all the effects.

Table 1 lists the parameter values calculated for each ensemble for both a 50 kt and 1 Mt explosion. Ignition threshold levels were defined for 10, 50, and 90% probabilities of ignition. Worst-case scenarios are represented by the negative standard deviation ensembles. Lower threshold levels corresponding to a greater slant range were used for positive standard deviation sets.

The mean visibility length (11 km) represents a clear day. Positive and negative unit standard deviations span the range of conditions from foggy to very clear days. In view of the uncertainty in the relations describing the transmittance of thermal radiation, mean values of the absorption α and scattering β coefficients were calculated from the average of the values given by EM-1 (4) and Brode (2). The lower estimates of α and β correspond to an increase in damage range and thus were used for the positive standard deviation ensembles. Values corresponding to the EM-1 (4) fit were used for the -1σ ensembles. Intermediate values were obtained by interpolating between the mean and $\pm 1\sigma$ sets.

For each ensemble, a degree of enhancement or attenuation of the incident thermal radiation was hypothesized. The values represent the likelihood of modification of the incident thermal radiation. The mean case postulates a greater probability of thermal radiation enhancement, but accounts for a lower probability of attenuation. The worst-case scenarios admit attenuation only and the standard deviation sets ($\geq 2/3\sigma$) admit enhancement only. To determine, for each ensemble, the adjusted incident radiation level necessary to produce a thermally induced ignition, the threshold radiation was divided by a modification factor

$$(1 + E_1)(1 + E_2)(1 - A)$$

where E_1 and E_2 represent the percentage enhancement of radiation by reflection from snow cover and a superior cloud deck. The quantity $(1 - A)$ defines the reduction of incident thermal radiation by cloud cover beneath the burst.

Target susceptibilities to blast-induced ignitions are defined for each ensemble using values suggested by Wilton, Myronuk, and Zaccor (5). The

Table 1--Ensembles of parameter values

Parameter	Parameter Value									
	-2 σ	- σ	-2/3 σ	-1/3 σ	Mean	+1/3 σ	+2/3 σ	+ σ	+2 σ	
50 kt ^a ignition threshold (cal/cm ²)										
90% probability	51	38	33	29	24	21	18	15	8	
50% probability	34	25	22	19	16	14	12	10	5	
10% probability	17	13	11	10	8	7	6	5	3	
1 Mt ^a ignition threshold (cal/cm ²)										
90% probability	60	47	42	37	33	30	27	25	18	
50% probability	40	31	28	25	22	20	18	17	12	
10% probability	20	16	14	12	11	10	9	9	6	
Visibility length (km)	2	5	7	9	11	22	35	46	92	
Transmissivity ^b										
α	3.2	2.9	2.75	2.60	2.45	2.30	2.15	2.0	1.8	
β	2.0	1.9	1.82	1.73	1.65	1.56	1.48	1.4	1.25	
Thermal radiation enhancement (Σ)										
Snow	--	--	--	--	10	30	50	70	90	
Clouds above	--	--	10	20	22	31	35	40	50	
Thermal radiation reduction (Σ)										
Clouds below	85	75	52	28	5	2	--	--	--	
Combined effects ^c	0.15	0.25	0.53	0.86	1.33	1.67	2.03	2.4	2.9	
Building type/contents indices for blast-induced fires	3/2.5	4/4	4.66/4.33	5.33/4.66	6/5	6.33/5.33	6.66/5.33	7/6	9/7.5	
Probable fire-spread enhancement factor	1.1	1.25	1.5	1.75	2.0	2.3	2.7	3.0	5.0	
Reduction of ignitions due to countermeasures (Δ)										
Thermally induced fires										
Overpressure \leq 0.5 psi	75	63	58	54	50	43	37	30	10	
Overpressure \leq 2 psi	50	33	31	28	25	22	18	15	5	
Overpressure \leq 5 psi	20	10	7	3	--	--	--	--	--	
Blast-induced fires										
Overpressure \leq 2 psi	80	60	53	47	40	35	30	25	10	
Overpressure \leq 5 psi	80	50	40	30	20	17	13	10	--	

^aHeight of burst = 500 ft/kt^{1/3}.

^b $[(1 + B(R/V)) \exp(-\alpha(R/V))]$.

^cThe multiplication factor is calculated as follows: threshold/combined effect = adjusted incident radiation.

building type index was varied from 3 (worst case, corresponding to heavy-design-load structures) to a +2 σ value of 9 (light wood-frame construction). Similarly, the contents type index assumes values from 2.5 (-2 σ ensemble) to 7.5. Average parameter values were used for the mean set.

An enhancement factor was used to determine the increased probability of a target ignition by fire spread. That factor was employed as a multiplication constant for each point in the fire-damage probability distribution. For the -2 σ set, fire spread increases the probability of fire damage by 10% and, for the +2 σ set, by 500%. The number of structure fires was doubled for the mean case.

The final two independent variables used in each ensemble accounted for the reduction in ignitions due to countermeasures. We distinguish countermeasures against thermally induced ignitions (e.g., reflective window coverings) from those against blast-induced ignitions (e.g., closure of central power and gas supplies). In both cases, the effectiveness of the countermeasures is assumed to be a function of the overpressure--lower overpressures mean fewer ignitions. We assume the countermeasures to be most effective

against the blast-induced ignitions. Their overall effectiveness decreases for the positive standard deviations.

Fire-damage-range curves representing the sum of the nine independent variables are shown in Fig. 6. The summation curves reflect the wide band of parameter values used to construct the ensemble. At the 50% damage level, the range from -2σ to $+2\sigma$ varies by a factor of 5. The damage range varies by a factor of 2 for the $\pm 1\sigma$ band.

The values selected for each variable were assumed to represent reasonable parameter choices. The positive standard deviation ensembles tend toward an expansion of the fire damage range. The negative ensembles represent a more conservative valuation. In all cases, each parameter choice is subject to confirmation by research. In constructing the ensembles, we chose values that should characterize a range of targets. Selection of a specific target or area should reduce the spread in values for threshold levels, building types/contents indices, and countermeasure effectiveness. Statistical definition of target area weather and local environmental conditions would establish a narrower range of visibility lengths and probabilities for thermal radiation enhancement or reduction. In any event, the mean, $\pm 1\sigma$, and $\pm 2\sigma$ damage-range curves should indicate the potential amount of fire damage.

SUMMARY

The sample fire damage-range curves presented in this paper estimate the immediate weapon effects-target response from blast and thermally induced ignitions as well as the longer time damage effects from those fires. Factors such as variable threshold levels, visibility lengths, transmissivity, cloud or snow cover, civil defense countermeasures, and blast induced ignitions were considered. A more complete survey is currently being prepared (3).

In many cases, simple linear predictive methods were used and parameter ranges created in order to estimate a particular effect. Though many approximations are used, the results should indicate the relative sensitivity of the damage-range curve to each effect. Improved estimates can be made as new theories are developed and parameter ranges refined. Topics not explicitly considered in the present study, but may warrant inclusion in further calculations include: blast-flame interactions, specific fire spread mechanisms, fire-wind damage beyond the fire periphery, variable urban structure, and multi-burst effects.

Specific target structures and cities are susceptible to complete destruction by fire. The damage curves and suggested uncertainty bands show that fires from nuclear weapon explosions are quantifiable and predictable. Conservative parameter valuations indicate that fire damage radii exceed those for blast damage. Less conservative--though realistic--parameter values greatly extend the probable fire damage radius. Verification of this trend would enable revision of current targeting and civil defense strategies.

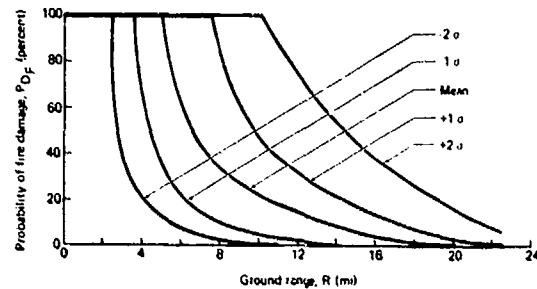


Fig. 6 Fire damage range for all parameters: summation curves, $W = 1$ Mt.

ACKNOWLEDGEMENT

This research was supported by the Defense Nuclear Agency and monitored by Dr. Michael J. Frankel.

REFERENCES

1. S. Glasstone and S. J. Dolan, The Effects of Nuclear Weapons, 3rd Ed., U.S. Department of Defense and the U.S. Department of Energy (1977).
2. H. L. Brode, Fireball Phenomenology, The Rand Corporation, Santa Monica, California, Report P3026 (1964).
3. H. L. Brode and R. D. Small, Fire Damage Estimations for Strategic Targeting, Pacific-Sierra Research Corporation, Los Angeles, California, In Press (1983).
4. Defense Nuclear Agency, Capabilities of Nuclear Weapons, (EM-1), Chapter 3, Part 1 (1972).
5. C. Wilton, D. Myronuk and J. Zaccor, Secondary Fire Analysis, Scientific Services, Inc., Redwood, City, California, Report 8048-6 (1981).
6. H. Bond (Ed.), Fire and the Air War, 1st Ed., National Fire Protection Association, Boston, Massachusetts (1951).
7. R. D. Small and H. L. Brode, Physics of Large Urban Fires, Pacific-Sierra Research Corporation, Los Angeles, California, PSR Report 1010 (March 1980).